# Role of uncoupling protein 1 and muscle AMP-activated protein kinase in diet-induced thermogenesis

**Kazuyo Takagi**

**Department of Physiological Science**

**School of Life Science**

**Graduate University for Advanced Studies (*SOKENDAI*)**

**2014**

**CONTENTS**


| | |
|---|---|
| **ABSTRACT** | **Page 2** |
| **INTRODUCTION** | **Page 5** |
| **METHODS** | **Page 8** |
| **RESULTS** | **Page 13** |
| **DISCUSSION** | **Page 19** |
| **ACKNOWLEDGEMENTS** | **Page 22** |
| **REFERENCE** | **Page 23** |
| **TABLES** | **Page 28** |
| **FIGURES** | **Page 30** |

**ABSTRACT**

Energy homeostasis is tightly regulated in mammals including humans, and their body weights are kept constant for a long interval. The measurement of food intake and energy expenditure (EE) is a central feature of studies attempting to investigate the homeostatic mechanism. However, analysis of total EE is complicated due to the presence of multiple biological processes that include the resting metabolic rate (RMR), EE induced by locomotor (muscle motor) activity (Ex) and diet-induced thermogenesis (DIT). Little study examined which process is involved in change in body weight in rodents as well as humans.

Brown adipose tissue (BAT) and skeletal muscle are important organs involved in regulation of energy homeostasis in mammals. BAT thermogenesis is regulated by the sympathetic nervous system (SNS) through the intracellular mechanism including β-adrenergic receptor, protein kinase A, lipolysis, and fatty acid-induced activation of mitochondrial uncoupling protein 1 (UCP1). UCP1 ablation induced obesity in mice fed laboratory chow (corn starch-based diet) as well as high-fat diet (HFD) when the mice were maintained at the thermoneutral environment (~30ºC for mice). However, the mice failed to induce obesity under "normal" animal house condition (i.e. 20-24ºC). The obesity-resistant phenotype of UCP1-gene ablated mice at the subthermoneutral environment was supposed to be due to the activation of compensatory mechanism in the mice.

An alternative site for the adaptive thermogenesis may be skeletal muscle, which involves both shivering and non-shivering thermogenesis (NST). Recent studies

revealed that $Ca^{2+}$-transport regulated by sarco/endoplasmic reticulum $Ca^{2+}$-ATPase pump (Serca) and its regulator sarcolipin involve NST in skeletal muscle, and ablation of sarcolipin caused obesity. AMP-activated protein kinase (AMPK) also plays an important role in glucose and lipid utilization in skeletal muscle during exercise and non-exercise. Previous studies revealed that leptin, an adipocyte hormone that plays a pivotal role in regulating energy homeostasis, activates AMPK and increases fatty acid oxidation in skeletal muscle, via directly acting on muscle and indirectly through the hypothalamic-SNS. However, the role of muscle AMPK in energy homeostasis remains elusive. Furthermore, it remains unknown whether AMPK involve the compensatory mechanism for the obesity-resistant phenotype of UCP1-ablated mice.

In the present study, I investigated the effect of ablation of UCP1 gene and suppression of AMPK activity in skeletal muscle in total EE in mice. First, I established the measurement of RMR, Ex and DIT in total EE. I found that total EE was highly co-related with locomotor activity in both fasting and feeding of HFD (high-calorie diet) after logarithmic conversion of the locomotor activity. Therefore RMR was determined with EE at the intercept on the y-axis of the linear regression during fasting. Ex at each time point in fasting and feeding was calculated with the linear regression line during fasting period. DIT was then obtained by subtracting Ex and RMR from total EE during HFD feeding.

Second, I examined each component (RMR, Ex and DIT) of total EE in UCP1 gene-ablated mice (UCP-KO), muscle-specific dominant negative-AMPK expressing mice (dnAMPK-mTg), and UCP1-KO and dnAMPK-mTg (KO-Tg) mice. Wild type

(WT) and KO-Tg mice were obtained by crossing UCP1-KO and dnAMPK-mTg mice. KO-Tg mice impaired DIT and total EE, but not RMR or Ex, compared with that of WT mice at the subthermoneutral environment (24ºC). KO-Tg mice significantly increased body weight even when the mice are pair-fed HFD with time-restricted feeding from 18:00-9:00, which protects HFD-induced obesity and metabolic abnormalities in WT mice. KO-Tg mice also caused glucose intolerance under lab chow feeding. UCP1-KO or dnAMPK-mTg mice did not alter EE, body weight or glucose metabolism.

Third, I found that KO-Tg mice abolished norepinephrine (NE)-induced increase in total EE. Furthermore, KO-Tg mice blunted NE-induced phosphorylation of AMPK and acetyl-CoA carboxylase (ACC), which is a target of AMPK, in muscle. In contrast, UCP1-KO mice enhanced NE-induced phosphorylation of AMPK and ACC in muscle. These results suggest that muscle AMPK involves a compensatory mechanism to regulate energy metabolism in UCP1-KO mice.

In conclusion, I found that muscle AMPK and UCP1 play an important role in energy homeostasis in mice. Muscle AMPK and UCP1 are both necessary to maintain in normal glucose metabolism in mice. Thus the present study provides a novel insight for important role of muscle AMPK as well as UCP1 in control of energy homeostasis.

## INTRODUCTION

Energy homeostasis is tightly regulated in mammals including humans, and their body weights are kept constant for a long interval. In a recent longitudinal study, for example, men with no history of obesity gained an average of only 0.18 kg body weight per year, suggesting the precise nature of the homeostatic system regulating energy balance (1). The measurement of food intake and energy expenditure (EE) is a central feature of studies attempting to investigate the homeostatic mechanism. However, analysis of total EE is complicated due to the presence of multiple biological processes that include the resting metabolic rate (RMR), EE induced by locomotor (muscle motor) activity (Ex) and diet-induced thermogenesis (DIT) (2). Little study examined which process is involved in change in body weight in rodents as well as humans.

Brown adipose tissue (BAT) and skeletal muscle are important organs involved in regulation of energy homeostasis in mammals (3). BAT thermogenesis is regulated by the sympathetic nervous system (SNS) through the intracellular mechanism including β-adrenergic receptor, protein kinase A, lipolysis, and fatty acid-induced activation of uncoupling protein 1 (UCP1) in mitochondria (4). Recent studies revealed that adult humans express active BAT and its thermogenic activity is negatively co-related with body mass index (5). Furthermore, white adipose tissues have been shown to express UCP1 in humans as well as rodents under environments such as cold exposure (6). Animal studies revealed that DIT is explained by adrenergic stimulation of the tissue (7). UCP1 ablation induced obesity in mice fed high-fat diet

(HFD) when the mice were maintained at the thermoneutral environment (~30ºC for mice) (7), whereas the mice failed to induce obesity under "normal" animal house condition (i.e. 20-24ºC) (8). UCP1 deficiency has also been reported to increase susceptibility of diet-induced obesity with aging at the subthermoneutral environment (9). The obesity-resistant phenotype of UCP1-gene ablated mice at the subthermoneutral environment was supposed to be due to the activation of compensatory mechanism in the mice (10).

An alternative site for the adaptive thermogenesis may be skeletal muscle, which involves both shivering and non-shivering thermogenesis (NST) (2, 11, 12). Recent studies showed that $Ca^{2+}$-transport regulated by sarco/endoplasmic reticulum $Ca^{2+}$-ATPase (Serca) pump and its regulator sarcolipin involve NST in skeletal muscle, and ablation of sarcolipin induced obesity at subthermoneutral environment (13, 14). AMP-activated protein kinase (AMPK) also plays an important role in glucose and lipid utilization in skeletal muscle during exercise and non-exercise (15, 16). Leptin, an adipocyte hormone that plays a pivotal role in regulating energy homeostasis, activates AMPK and increases fatty acid oxidation in skeletal muscle, via directly acting on muscle and indirectly through the hypothalamic-SNS (17). However, the role of muscle AMPK in energy homeostasis remains elusive.

In the present study, I investigated the effect of ablation of UCP1 gene and suppression of AMPK activity in skeletal muscle in total EE in mice. First, I established the measurement of RMR, Ex and DIT in total EE in individual mice. Second, I found that mice which suppressed both UCP1 and muscle AMPK activity, impaired DIT and

total EE, but not RMR or Ex, and resulted in obesity even when the mice are pair-fed HFD at the subthermoneutral environment (24ºC). KO-Tg mice also impaired glucose tolerance. Third, I found that KO-Tg mice blunted norepinephrine (NE)-induced thermogenesis, as well as NE-induced phosphorylation of muscle AMPK and acetyl-CoA carboxylase (ACC) (18). In contrast, UCP1 gene-ablated (UCP1-KO) mice increased NE-induced phosphorylation of AMPK activation and ACC in skeletal muscle, suggesting that muscle AMPK involves obesity-resistant phenotype of UCP1-KO mice.

## RESEARCH DESIGN AND METHODS

### Animals

All animal experiments were performed in accordance with institutional guidelines for the care and handling of experimental animals, and they were approved by the Institutional Animal Care and Use Committee (IACUC) of National Institutes of Natural Sciences. UCP1-KO mice (8) were kindly provided by Dr. Yamashita (Chubu University, Japan) and Dr. Kozak (Institute of Animal Reproduction and Food Research of the Polish Academy of Sciences, Poland). Skeletal muscle-specific dominant negative AMPK expressing (dnAMPK-mTg) mice were provided by Dr. Miura (University of Shizuoka, Japan) and Dr. Ezaki (Showa Women's University, Japan) (19). dnAMPK-mTg mice were overexpressed mutated α1 catalytic subunit of AMPK, which is changed the residue asparagic acid at $157^{th}$ to alanine (Asp157Ala), preferentially in skeletal muscle under the control of α-skeletal actin promoter (19). ASP 157 lies in the conserved DFG (subdomain VII in the protein kinase catalytic subunit) motif, which is essential for $Mg^{2+}$-ATP biding in protein kinases (19). UCP1-gene ablated and dnAMPK-mTg expressing (KO-Tg) mice and their wild type (WT) mice were obtained by crossing dnAMPK-mTg and UCP1-KO mice. The animals were housed individually in plastic cages at 24 ± 1ºC with lights on from 6:00 to 18:00 hour, and they were maintained with free access to a laboratory chow (CE-2, CLEA Japan, Tokyo, Japan). Male mice of 15-20 weeks of age were used, except that 10-38 weeks of age of mice were used to study body weight change during HFD feeding.

**Indirect calorimetry**

Total energy expenditure (EE), RMR, Ex and DIT were measured by indirect calorimetry with use of a gas analysis consisting $CO_2$ and $O_2$ mass spectrometric analyzer (Arco-2000, Arco System, Chiba, Japan). Locomotor activity (cm/min) was simultaneously measured with force plate system that was set below the animal cage (Actracer-2000, Arco system). Force plate system detects low-intensity activities such as grooming and shivering (2). EE and the amount of carbohydrate or fat oxidized were calculated from $O_2$ consumption ($VO_2$) and $CO_2$ production ($VCO_2$) as described previously (20). Equations for those calculations were as follows:

EE (cal/min) $=3.816\times VO_2$ (L) $+ 1.231\times VCO_2$ (L)  (L: liter)

Carbohydrate oxidation (g/min) $=(4.51\times VCO_2)-(3.18\times VO_2)$

Lipid oxidation (g/min) $= 1.67(VO_2-VCO_2)$

Mice were adapted in the individual cage for indirect calorimetry over 2-days. $VO_2$, $VCO_2$ and locomotor activity were measured every minute, and the data were averaged for every consecutive 5 min or 1 hour. To determine RMR, mice were deprived of foods from 9:00, and measurements were continued until 9:00 on the next day (Fasting experiment). To minimize the effect of foods, data from 14:00 to 9:00 (“fasting period”) were used for calculation of RMR. To determine DIT, mice were deprived of foods from 9:00, and refed HFD (D12492, Research Diets, New Brunswick, NJ) at 18:00 (feeding experiment). DIT was calculated with the data from 18:00 to 9:00 (“feeding period”).

**Calculation of RMR, Ex and DIT**

Consistent with a previous study (2), I found that total EE was highly co-related with logarithmically converted locomotor activity in both fasting and feeding experiments in individual mice (see RESULTS). RMR was then determined with EE at the intercept on the y-axis of the linear regression in fasting experiments. Ex at each time point in fasting and feeding experiments was calculated with the logarithmically converted locomotor activity and the slope of the linear regression line in fasting experiment. DIT was calculated by subtracting Ex and RMR from total EE during feeding period (18:00 to 9:00).

**NE injection**

Mice were deprived of foods from 9:00, and NE (1 mg/kg body weight, L-(−)-Norepinephrine (+)-bitartrate salt monohydrate, Sigma Aldrich, St. Louis, Mo) was subcutaneously (s.c.) injected into the conscious and unrestrained mice at 18:00. Control mice were injected saline s.c. $VO_2$ and $VCO_2$ were measured from -20 min to 100 min after NE injection. In different experiment, some mice were euthanatized at 30 min after NE infusion and collected tissues samples for biochemical analysis.

**Long-term feeding of HFD**

Previous study revealed that mice with time-restricted feeding during night period were protected against obesity and metabolic abnormalities induced by HFD feeding (21). Therefore, mice were fed HFD (D12492, Research Diets) during a restricted time period

from 18:00 to 9:00. Mice were also pair-fed to minimize the effect of different amount of food intake on total EE.

**Glucose tolerance test (GTT)**

After overnight fasting, animals were injected glucose (1 g/kg) intraperitoneally (i.p.). Blood was collected from the tail at 0, 10, 30, 60, 90, and 120 min after glucose injection. Plasma concentrations of glucose and insulin were measured with kits as described below.

**Immunoblot analysis**

Tissues were homogenized at 4°C in 20 mM Tris (pH 7.4), 5 mM EDTA (pH 8.0), 10 mM sodium pyrophosphate, 1% Triton X, phosphatase inhibitor (Calbiochem, California, USA) and proteinase inhibitor (Sigma). The homogenates were centrifuged, and the resulting supernatants (10 μg of protein) were fractionated by SDS-PAGE. Immunoblot analysis was then performed with specific antibodies as indicated Table 2. Immune complexes were visualized with horseradish peroxidase–conjugated secondary antibodies (Anti IgG, Santa Cruz Biotechnology, California, USA) and enhanced chemiluminescence reagents (GE Healthcare, Tokyo, Japan). Protein bands were quantified using CS Analyzer ver 3.0 ATTO densitograph software (ATTO CORP., Tokyo, Japan).

**Measurement of plasma metabolites and hormone**

Plasma concentrations of glucose (Glucose CII-test, Ca. No. 439-90901, Wako, Osaka, Japan), nonestrified free fatty acids (NEFA) (NEFA C-test, Ca. No. 279-75401, Wako, Osaka, Japan), triglycerides (TG) (Triglyceride E-test, Ca. No. 432-40201, Wako, Osaka, Japan), insulin (Mouse Insulin ELISA KIT (U-type), Ca. No. AKRIN-031, Shibayagi, Gunma, Japan) in blood samples were measured by the kits as described.

**Statistical analysis**

Data are presented as means ± standard error of the mean (SEM). Statistical comparisons among multiple groups were performed by analysis of variance (ANOVA) followed by Tukey-Kramer's post hoc test. Statistical analysis between 2 groups was performed by Student's t test. A P value of $<0.05$ was considered statistically significant.

## RESULTS

### Measurements of RMR, Ex and DIT in individual mice

I first established the measurement of RMR, Ex and DIT in individual mice. Total EE was measured in WT mice under two feeding conditions: when mice were deprived of foods from 9:00 to 9:00 (Fig. 1A) and when mice were refed HFD from 18:00 to 9:00 (Fig. 1B). Fig. 1C and D show the results in a representative WT mouse in fasting and feeding experiments, respectively. I found that sharp increase in total EE was associated with increased locomotor activity during fasting (Fig. 1C). Similar pattern was observed during feeding. However, correlation between individual peak of total EE and increase in locomotor activity appeared to be weaker than that during fasting. Fig. 1C and D showed basal level of EE decreased during fasting, while that of EE increased after refeeding.

Fig. 1E and F revealed a close correlation between total EE and locomotor activity from 14:00 to 9:00 in the mouse. Total EE was highly correlated with locomotor activity after logarithmic conversion in both fasting and feeding experiments (Table 1). High value of $R^2$ in fasting experiments (>0.63) suggested that difference of total EE at each time point during fasting is explained with the change in locomotor activity. Thus RMR in individual mice was determined with EE at the intercept (b) on the y-axis of the regression line in fasting experiment (data from14:00 to 9:00) (Fig. 1E and G). The correlated component in total EE with locomotor activity in fasting experiment was

defined as Ex (Fig. 1H). Ex at each time point was calculated with the slope (a) of the regression.

Relatively lower value of $R^2$ in refeeding experiments (<0.62) than that in fasting experiments suggests that total EE during refeeding contains a component not explained by locomotor activity. Furthermore, total EE at the intercept on y-axis of the regression in refeeding experiments was higher than that in fasting experiments (Fig. 1E-G and Table 1). Thus, DIT includes all components of EE that exceeded Ex plus RMR (Fig. 1H). Interestingly, the slope (a) was not different in fasting and refeeding experiments (Fig. 1E-G and Table1), suggesting that refeeding and fasting did not change energy efficiency of locomotor activity or shivering, partly due to that movements of mice were restricted in small cages for the indirect calorimetry.

**Expression and phosphorylation of AMPK and UCP1 in UCP1-KO, dnAMPK-mTg, and KO-Tg mice**

I examined expression and phosphorylation of AMPK and ACC in skeletal muscle in UCP1-KO, dnAMPK-mTg, and KO-Tg mice fed lab chow ad libitum (Fig. 2A). As reported previously (19), amount of α1 catalytic subunit of AMPK and phosphorylation (Thr172) increased in soleus muscle in dnAMPK-mTG and KO-Tg mice by muscle-specific overexpression of α1-mutated subunit (Fig. 2A). In contrast, amount of α2 catalytic subunit of AMPK decreased in the muscle in these mice, probably due to the reason that single subunit of AMPK not consisted of heterotrimer are degraded (19). In parallel to the overexpression of mutant α1 subunit, phosphorylation of ACC (Ser79

and Ser81 for ACC1 and ACC2, respectively) (18), a down-stream target of AMPK, tended to decrease in soleus muscle in dnAMPK-mTg and KO-Tg mice, but not UCP1-KO mice, without change in total amount of the protein. The amount of UCP1 protein was not detected in UCP1-KO and KO-Tg mice. dnAMPK-mTg mice did not alter the UCP1 protein expression in BAT.

**Correlation and regression of total EE against locomotor activity in UCP1-KO, dnAMPK-mTg, and KO-Tg mice**

Body weight did not differ among groups when mice were fed lab chow ad libitum (Table 1). Pair-feeding of HFD equaled amounts of accumulated food intake among groups (Table 1). I examined the slope (a) and intercept on the y-axis of the regression for total EE against locomotor activity (Table 1). The slope (a) was not different among groups in either fasting or feeding. The results suggested that energy efficiency of muscle motor activity was not changed by suppression of UCP1 or muscle AMPK. EE at the intercept on y-axis (b) in fasting experiment (i.e. RMR) was not different among groups (Table 1 and see Fig. 2E). EE at the intercept in refeeding experiment tended to be higher than that during fasting but it was not statistically significant (Table 1).

**DIT as well as total EE is decreased in KO-Tg mice**

I investigated change in total EE during feeding (Fig. 2B and C). Total EE during refeeding of HFD (18:00 to 9:00) was increased in all groups (Fig. 2B). Calorie intake of HFD was higher than that of lab chow, and the increase in total EE was higher than

that of lab chow (data not shown). Thus, total EE was increased by feeding, dependent on the calorie and nutrients in the foods. Total EE during HFD feeding was gradually decreased in KO-Tg mice, compared with that in WT mice (Fig. 2B). Sum of the total EE during feeding was significantly lower in KO-Tg mice than that in WT mice (Fig. 2C). Total EE during fasting and RMR were not different among groups (Fig. 2D, 2E and intercept on y-axis during fasting in Table 1). Locomotor activity (data not shown) and Ex were also not different among groups (Fig. 2F and G). In contrast, DIT significantly decreased in KO-Tg mice, compared with other groups (Fig. 2H and I).

**NE-induced thermogenesis is impaired in KO-Tg mice**

UCP1 and muscle AMPK are regulated by the SNS. I examined NE-induced thermogenesis in those groups. Mice were deprived of foods from 9:00, and NE was subcutaneously injected at 18:00 (Fig. 3A). NE increased total EE in WT, dnAMPK-mTg, and UCP1-KO mice, but did not in KO-Tg mice (Fig. 3B and C). The increase in total EE in UCP1-KO mice tended to be lower than that of WT mice (Fig. 3B). dnAMPKmTg mice also decreased the increase in total EE during 45 to 60 min (Fig. 3B), while sum of the total EE was not significantly different from that of WT mice (Fig. 3C).

I examined whether KO-Tg mice changed NE-induced carbohydrate or lipid oxidation (Fig. 3D and E). WT, UCP1-KO, and dnAMPK-mTg mice, but not dnAMPK-mTg mice, significantly increased lipid oxidation. Carbohydrate oxidation was significantly lower than lipid oxidation in all groups, and suppressed by NE

injection in UCP1-KO, dnAMPK-mTg, and KO-Tg mice. The suppression of carbohydrate oxidation is probably due to NE-induced lipolysis in those mice.

**Enhancement of NE-induced activation of muscle AMPK in UCP1-KO mice**

I next examined NE-induced phosphorylation of AMPK and ACC in skeletal muscle (Fig. 3F and G). UCP1-KO mice increased NE-induced phosphorylation (Thr172) of AMPK in soleus muscle, compared with that of WT mice (Fig. 3F). dnAMPK-mTg and KO-Tg mice did not increase the phosphorylation of AMPK significantly, due to the increased phosphorylation of overexpressed mutant α1 subunit of AMPK at the basal level (data not shown).

ACC is a target of AMPK, and regulates fatty acid oxidation in mitochondria (18). In parallel to the AMPK phosphorylation, UCP1-KO mice increased the NE-induced phosphorylation of ACC compared with that in WT mice (Fig. 3G). In contrast, dnAMPK-mTg or KO-Tg mice did not increase the phosphorylation of ACC significantly. These results suggested that ablation of UCP1 gene augmented the NE-induced phosphorylation of AMPK and ACC in soleus muscle.

**KO-Tg mice induce obesity at the subthermoneutral environment.**

My results revealed that KO-Tg and dnAMPK-mTg mice decrease DIT and total EE at the subthermoneutral environment. I therefore examined whether KO-Tg mice induce obesity with HFD feeding. Mice were pair-fed HFD with time-restricted schedule (Fig. 4A) that has been shown to protect HFD-induced obesity and metabolic abnormalities

in WT mice (21). Therefore, the amount of accumulated food intake was not different among groups (Fig. 4B). Nevertheless, KO-Tg mice, but not UCP1-KO or dnAMPK-mTg mice, increased body weight compared with that of WT mice (Fig. 4C and D). Given that the increase in body weight was almost due to the enlargement of white adipose tissue (7 kcal/g tissue weight), the body weight increase in KO-Tg mice was explained by the sum of the decrease of DIT during HFD feeding (Fig. 2)

**Impairment of glucose and lipid metabolism in KO-Tg mice**

I examined whether KO-Tg mice change glucose metabolism (Fig. 5A and B). KO-Tg mice showed glucose intolerance during GTT even when the mice were kept with lab chow ad libitum (Fig. 5A). UCP1-KO mice tended to be glucose-intolerant, but it was not significant. dnAMPK-mTg mice did not alter glucose tolerance. Plasma insulin levels tended to increase in KO-Tg and UCP1-KO mice but not in dnAMPK-mTg mice (Fig. 5B). Basal level of plasma glucose was not different among groups either when fed lab chow ad libitum or pair-fed HFD with time-restricted feeding schedule (Fig. 5C and D). In contrast, plasma insulin level was significantly higher in KO-Tg mice when fed HFD (Fig. 5E and F). KO-Tg mice also increased plasma concentration of NEFA (Fig. 5G) but not TG (Fig. 5H). Thus, KO-Tg mice, but not UCP1-KO or dnAMPKmTg mice, induced obesity and impaired glucose and fatty acid metabolism.

## DISCUSSION

In the present study, I examined the role of UCP1 and muscle AMPK in energy homeostasis in mice. I found that suppression of both UCP1 and muscle AMPK activity decreased DIT and total EE, and resulted in obesity with HFD feeding at the subthermoneutral environment. Previous study revealed that UCP1-KO mice induced obesity at thermoneutral (7) but not at subthermoneutral environment (8), probably due to the activation of the compensatory mechanism in the mice. My results thus suggest that muscle AMPK as well as UCP1 plays an important role in the regulation of energy homeostasis in mice. I also found that suppression of both UCP1 and muscle AMPK activity impairs glucose and lipid metabolism even when the mice are fed lab chow ad libitum or when pair-fed HFD with time-restricted feeding schedule.

Total EE is composed of RMR, Ex and DIT (2). However, little study examined which process is involved in change in body weight in experimental animals as well as humans. I examined the measurement of RMR, Ex and DIT in individual mice. I found that total EE was highly correlated with locomotor activity after logarithmic conversion in both fasting and feeding experiments. Thus, RMR and Ex were determined by the linear regression line during fasting. DIT was calculated by subtracting RMR and Ex from total EE during feeding. DIT might include change in energy efficiency of shivering and muscle motor activity with HFD feeding. However, it is unlikely because the slope (a) of the linear regression line was not different between fasting and refeeding experiments.

AMPK in skeletal muscle regulates glucose and lipid utilization in the tissue during exercise and non-exercise (15, 16, 17). Previous studies revealed that leptin activates AMPK and increases fatty acid oxidation in skeletal muscle, via directly acting on muscle and indirectly through the hypothalamic-SNS (17). Muscle AMPK is activated by calcium/calmodulin-dependent protein kinase kinase (CaMKK) or LKB1. Activation of AMPK phosphorylates ACC and decreases malonyl-CoA concentration. Decrease of malonyl-CoA level activates mitochondrial fatty acid oxidation through deinhibition of carnitine palmitoyltransferase (CPT) 1 activity. AMPK also activates peroxisome proliferator-activated receptor gamma co-activator 1α (PGC1α), which induces an upregulation of mitochondrial gene expression and mitochondriogenesis (22, 23). Thus, energy production by AMPK-induced fatty acid oxidation in skeletal muscle may be important for DIT in response to HFD feeding. Impairment of fatty acid utilization in skeletal muscle and BAT probably resulted in glucose intolerance in KO-Tg mice thorough the “lipotoxicity” in those tissues (24). A nucleotide polymorphism in gene encoding α1 or α2 subunits of AMPK is associated with the susceptibility to type II diabetes (25) and the response of anti-diabetic drug metformin in humans (26).

Skeletal muscle involves shivering and non-shivering thermogenesis (3). It is unlikely that shivering thermogenesis decreased in KO-Tg mice, because Ex as well as the slope (a) of the regression line for total EE against locomotor activity did not change in the mice. Metabolic abnormalities including insulin resistance caused by suppression of muscle AMPK and UCP1 may contribute to the decrease of DIT in KO-Tg mice.

However, my finding showing that UCP1 gene ablation enhanced NE-induced activation of muscle AMPK supported the hypothesis that muscle AMPK plays an important role in SNS-regulated thermogenesis and compensatory mechanism in UCP1-KO mice. Sarcolipin gene-ablated mice revealed that $Ca^{2+}$-transport regulated by sarco/endoplasmic reticulum $Ca^{2+}$-ATPase (Serca) pump in skeletal muscle involves adaptive thermogenesis in mice (13, 14). It is interesting to examine the role of AMPK in serca and sarcolipin-regulated thermogenesis in skeletal muscle.

The present study showed that NE-induced thermogenesis is slightly impaired in UCP1-KO and dnAMPK-mTg mice (Fig. 3A). Thus, decrease of DIT in KO-Tg mice might be due to the additive effects of impairment of thermogenesis derived by UCP1 and muscle AMPK. However, the finding that UCP1 gene ablation enhanced NE-induced activation of AMPK in skeletal muscle, suggests a cooperative action on UCP1 and muscle AMPK-induced thermogenesis. It is possible that BAT or UCP1-expressing white adipose tissue releases some adipokine that affects SNS-induced activation of muscle AMPK and its thermogenesis (27). Furthermore, dnAMPK-mTg mice may activate or induce compensatory mechanism to keep energy balance in the mice.

UCP1 plays a crucial role in NST in small rodents (4, 5). Recent studies revealed that human adults, although not all, also express thermogenically active BAT (5). Metabolic activity of BAT was negatively correlated with the body mass index in humans (5). Recent studies suggested that UCP1 expresses in white adipose tissues in humans as well as in small rodents under some environmental condition such as cold

exposure (9). However, it still remains unclear how much BAT thermogenesis contributes to energy homeostasis in humans. Energy efficiency in muscle thermogenesis is lower than that of BAT (28), and therefore large amount of energy substrates are consumed for the thermogenesis. Therefore, muscle thermogenesis might be protective to diet-induced obesity and metabolic abnormalities. Given that relative amount of muscle is larger in humans than that in small rodents, muscle AMPK, as well as UCP1, is probably important in the control of energy and metabolic homeostasis in humans.

In conclusion, I found that muscle AMPK plays an important role in total EE in mice in synergic action with UCP1. Furthermore, muscle AMPK and UCP1 were necessary to maintain in normal glucose and lipid metabolism in mice. Thus, the present study provides a novel insight for important role of muscle AMPK as well as UCP1 in the control of energy and metabolic homeostasis.

**ACKNOWLEDGMENTS**

I would like to express my sincere appreciation to Drs. Yasuhiko Minokoshi, Shiki Okamoto, Chitoku Toda for their generous supports and valuable guidance trough this study. I would also like to thank Kumiko Saito and Megumi Hayashi for helpful assistance. I would also like to thank Dr. Yamashita, Dr. Kozak, Dr. Miura and Dr. Ezaki for kindly providing UCP1-KO mice and dnAMPK-mTg mice. I wish to thank all the member of Division of Endocrinology and Metabolism for their supports, and inspiring discussion.

**REFERENCES**


1. Van Wye G, Dubin JA, Blair SN, Dipietro L. Adult obesity does not predict 6-year weight gain in men: the Aerobics Center Longitudinal Study. *Obesity (Silver Spring).* 15: 1571–1577, 2007
2. Virtue S1, Even P, Vidal-Puig A. Below thermoneutrality, changes in activity do not drive changes in total daily energy expenditure between groups of mice. *Cell Metab.* 16: 665-671, 2012.
3. Himms-Hagen J. Exercise in a pill: feasibility of energy expenditure targets. *Curr Drug Targets CNS Neurol Disord.* 3: 389-409, 2004.
4. Cannon B, Nedergard J. Brown adipose tissue: function and physiological significance. *Physiol Rev*. 84: 277–359, 2004.
5. Saito M. Human brown adipose tissue: regulation and anti-obesity potential. *Endocr J.* 61: 409-416, 2014.
6. Rosen ED, Spiegelman BM. What we talk about when we talk about fat. *Cell*. 156: 20-44, 2014.
7. Feldmann HM, Golozoubova V, Cannon B, Nedergaard J. UCP1 ablation induces obesity and abolishes diet-induced thermogenesis in mice exempt from thermal stress by living at thermoneutrality. *Cell Metab.* 9: 203-209, 2009.
8. Enerbäck S, Jacobsson A, Simpson EM, Guerra C, Yamashita H, Harper ME, Kozak LP. Mice lacking mitochondrial uncoupling protein are cold-sensitive but not obese. *Nature* 387: 90-94, 1997.

9. Kontani Y, Wang Y, Kimura K, Inokuma KI, Saito M, Suzuki-Miura T, Wang Z, Sato Y, Mori N, Yamashita H. UCP1 deficiency increases susceptibility to diet-induced obesity with age. *Aging Cell*. 4: 147-155, 2005.
10. Liu X, Rossmeisl M, McClaine J, Riachi M, Harper ME, Kozak LP. Paradoxical resistance to diet-induced obesity in UCP1-deficient mice. *J Clin Invest*. 111: 399-407, 2003.
11. Lowell B, Spiegelman BM. Towards a molecular understanding of adaptive thermogenesis. *Nature.* 404: 652-660, 2000.
12. Tseng YH, Cypess AM, Kahn CR. Cellular bioenergetics as a target for obesity therapy. *Nat Rev Drug Discov*. 9: 465-82, 2010.
13. Bal NC, Maurya SK, Sopariwala DH, Sahoo SK, Gupta SC, Shaikh SA, Pant M, Rowland LA, Bombardier E, Goonasekera SA, Tupling AR, Molkentin JD, Periasamy M. Sarcolipin is a newly identified regulator of muscle-based thermogenesis in mammals. *Nat Med* 18: 1575-1579, 2012.
14. Bombardier E, Smith IC, Gamu D, Fajardo VA, Vigna C, Sayer RA, Gupta SC, Bal NC, Periasamy M, Tupling AR. Sarcolipin trumps β-adrenergic receptor signaling as the favored mechanism for muscle-based diet-induced thermogenesis. *FASEB J.* 27: 3871-3878, 2013.
15. Richter EA, Hargreaves M. Exercise, GLUT4, and skeletal muscle glucose uptake. *Physiol Rev*. 93: 993-1017, 2013.
16. Dzamko NL, Steinberg GR. AMPK-dependent hormonal regulation of whole-body energy metabolism. *Acta Phsiol (Oxf)*. 196: 115-127, 2009.

17. Minokoshi Y, Kim YB, Peroni OD, Fryer LG, Müller C, Carling D, Kahn BB. Leptin stimulates fatty-acid oxidation by activating AMP-activated protein kinase. *Nature*. 415: 339-343, 2002.
18. Fullerton MD, Galic S, Marcinko K, Sikkema S, Pulinilkunnil T, Chen ZP, O'Neill HM, Ford RJ, Palanivel R, O'Brien M, Hardie DG, Macaulay SL, Schertzer JD, Dyck JR, van Denderen BJ, Kemp BE, Steinberg GR. Single phosphorylation sites in Acc1 and Acc2 regulate lipid homeostasis and the insulin-sensitizing effects of metformin. *Nat Med*. 19: 1649-1654, 2013.
19. Miura S, Kai Y, Kamei Y, Bruce CR, Kubota N, Febbraio MA, Kadowaki T, Ezaki O. Alpha2-AMPK activity is not essential for an increase in fatty acid oxidation during low-intensity exercise. *Am J Physiol Endocrinol Metab*. 296: E47-E55, 2009.
20. Ishihara K, Oyaizu S, Onuki K, Lim K, Fushiki T. Chronic (-)-hydroxycitrate administration spares carbohydrate utilization and promotes lipid oxidation during exercise in mice. *J Nutr*. 130: 2990-2995, 2000.
21. Hatori M, Vollmers C, Zarrinpar A, DiTacchio L, Bushong EA, Gill S, Leblanc M, Chaix A, Joens M, Fitzpatrick JA, Ellisman MH, Panda S. Time-restricted feeding without reducing caloric intake prevents metabolic diseases in mice fed a high-fat diet. *Cell Metab*. 15: 848-860, 2012.
22. Iwabu M, Yamauchi T, Okada-Iwabu M, Sato K, Nakagawa T, Funata M, Yamaguchi M, Namiki S, Nakayama R, Tabata M, Ogata H, Kubota N, Takamoto I, Hayashi YK, Yamauchi N, Waki H, Fukayama M, Nishino I, Tokuyama K, Ueki K, Oike Y, Ishii S, Hirose K, Shimizu T, Touhara K, Kadowaki T. Adiponectin and AdipoR1 regulate

PGC-1alpha and mitochondria by $Ca^{2+}$ and AMPK/SIRT1. *Nature*. 464: 1313-1319, 2010.

23. Cantó C, Gerhart-Hines Z, Feige JN, Lagouge M, Noriega L, Milne JC, Elliott PJ, Puigserver P, Auwerx J. AMPK regulates energy expenditure by modulating $NAD^{+}$ metabolism and SIRT1 activity. *Nature*. 458: 1056-1060, 2009.
24. Osborn O, Olefsky JM. The cellular and signaling networks linking the immune system and metabolism in disease. *Nat Med*. 18: 363-374, 2012.
25. Jablonski KA, McAteer JB, de Bakker PI, Franks PW, Pollin TI, Hanson RL, Saxena R, Fowler S, Shuldiner AR, Knowler WC, Altshuler D, Florez JC; Diabetes Prevention Program Research Group. Common variants in 40 genes assessed for diabetes incidence and response to metformin and lifestyle intervention in the diabetes prevention program. *Diabetes*. 59: 2672-2681, 2010.
26. Keshavarz P, Inoue H, Nakamura N, Yoshikaand, Tanahashi T, Itakura M. Single nucleotide polymorphisms in genes encoding LKB1 (STK11), TORC2 (CRTC2) and AMPK alpha2-subunit (PRKAA2) and risk of type 2 diabetes. *Mol Genet Metab*. 93: 200-209, 2008.
27. Villarroya J, Cereijo R, Villarroya F. An endocrine role for brown adipose tissue? *Am J Physiol Endocrinol Metab*. 305: E567-E572, 2013.
28. Kozak LP. Brown fat and the myth of diet-inducd thermogenesis. *Cell Metab*. 11: 263-267, 2010.
29. Suzuki A, Okamoto S, Lee S, Saito K, Shiuchi T, Minokoshi Y. Leptin stimulates fatty acid oxidation and peroxisome proliferator-activated receptor alpha gene expression

in mouse C2C12 myoblasts by changing the subcellular localization of the alpha2 from of AMP-activated protein kinase. *Mol Cell Biol*. 27: 4317-4327, 2007.

**Table 1.** Body weight, food intake during HFD feeding, and linear regression parameters for total EE against locomotor activity.

| | | **WT** (*n*=9) | **UCP1-KO** (*n*=9) | **dnAMPK-mTg** (*n*=10) | **KO-Tg** (*n*=10) |
|---|---|---|---|---|---|
| Body weight (g) | | 30.1 ± 0.5 | 31.1 ± 1.7 | 30.6 ± 0.9 | 29.1 ± 0.8 |
| Food intake (kcal/18:00-9:00) | | 21.2 ± 0.6 | 20.2 ± 1.6 | 21.7 ± 0.6 | 19.6 ± 0.6 |
| $R^2$ | Fasted | 0.65 ± 0.02 | 0.63 ± 0.02 | 0.67 ± 0.04 | 0.69 ± 0.01 |
| | HFD | 0.60 ± 0.03 | 0.55 ± 0.03 | 0.55 ± 0.03 | 0.57 ± 0.02 |
| Slope (a) | Fasted | 2.2 ± 0.1 | 2.0 ± 0.1 | 2.1 ± 0.1 | 2.0 ± 0.1 |
| | HFD | 2.3 ± 0.1 | 2.2 ± 0.2 | 2.3 ± 0.1 | 2.1 ± 0.1 |
| Intercept on y-axis (b) | Fasted | 4.2 ± 0.1 | 4.5 ± 0.3 | 3.9 ± 0.1 | 4.0 ± 0.1 |
| | HFD | 6.0 ± 0.2* | 5.6 ± 0.3* | 5.4 ± 0.2* | 5.3 ± 0.4* |

1) Body weight on the day of EE measurement.
2) Food intake during refeeding of HFD (18:00 to 9:00)
3) Parameters (a and b) of linear regression line (y=ax+b) for total EE against logarithmically converted locomotor activity (14:00-9:00) in fasting and HFD refeeding experiments.

*$p<0.05$ vs fasted.

**Table 2.** List of antibodies

| Antibody name | Catalog No. | Company name | Dilution |
|---|---|---|---|
| phospho AMPKα (Thr172) | 2531 | Cell Signaling Technology | 1 to 1000 |
| total AMPKα | 2532 | Cell Signaling Technology | 1 to 1000 |
| α1 subunit of AMPK | Affinity-purified antibody made originally[29)] | | 1 to 5000 |
| α2 subunit of AMPK | ab3760 | Abcam | 1 to 1000 |
| Acetyl CoA Carboxylase Antibody | 3662 | Cell Signaling Technology | 1 to 1000 |
| phospho Acetyl CoA Carboxylase (ser79) Antibody | 3661 | Cell Signaling Technology | 1 to 1000 |
| UCP1 | ab23841 | Abcam | 1 to 1000 |
| Anti IgG, Rabbit (Goat) | SC3837 | Santa Cruz Biotechnology | 1 to 2000 |

Cell Signaling Technology, Danvers, MA, USA

Abcam, Boston MA, USA

Santa Cruz Biotechnology, California, USA

# Figure 1

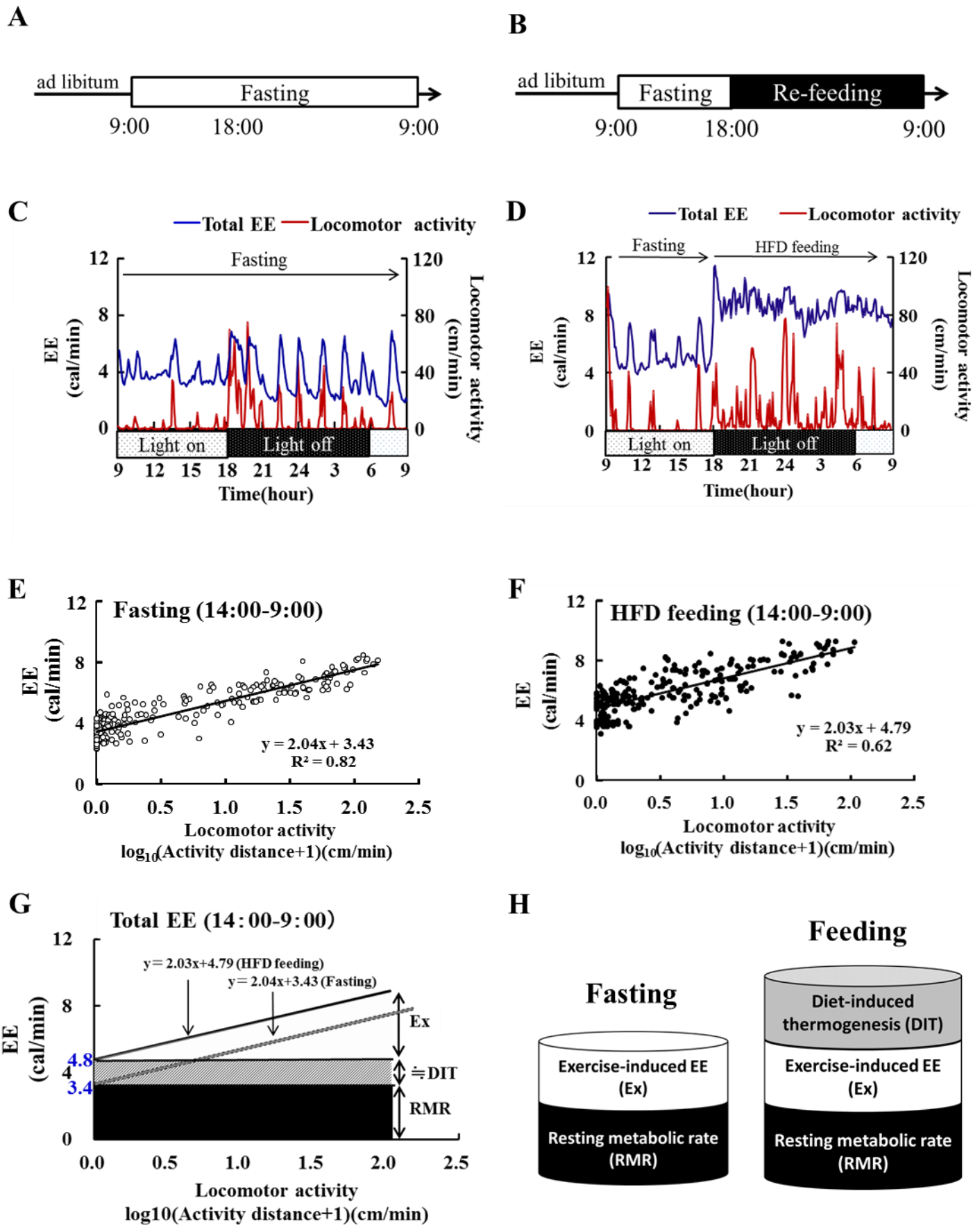
A
ad libitum
Fasting
9:00
18:00
9:00
B
ad libitum
Fasting
Re-feeding
9:00
18:00
9:00
C
Total EE
Locomotor activity
Fasting
EE (cal/min)
Locomotor activity (cm/min)
Light on
Light off
Time(hour)
D
Total EE
Locomotor activity
Fasting
HFD feeding
EE (cal/min)
Locomotor activity (cm/min)
Light on
Light off
Time(hour)
E
Fasting (14:00-9:00)
EE (cal/min)
y = 2.04x + 3.43
R² = 0.82
Locomotor activity
log10(Activity distance+1)(cm/min)
F
HFD feeding (14:00-9:00)
EE (cal/min)
y = 2.03x + 4.79
R² = 0.62
Locomotor activity
log10(Activity distance+1)(cm/min)
G
Total EE (14:00-9:00)
y= 2.03x+4.79 (HFD feeding)
y= 2.04x+3.43 (Fasting)
EE (cal/min)
4.8
3.4
Ex
≒DIT
RMR
Locomotor activity
log10(Activity distance+1)(cm/min)
H
Feeding
Fasting
Diet-induced thermogenesis (DIT)
Exercise-induced EE (Ex)
Resting metabolic rate (RMR)
Exercise-induced EE (Ex)
Resting metabolic rate (RMR)

Figure 1. Measurements of RMR, Ex and DIT in individual mice.

(A, B) Experimental schedule in fasting (A) and refeeding (B) experiments. Mice were refed HFD at 18:00 in refeeding experiment (B).

(C, D) Total EE and locomotor activity in a representative mouse in fasting and refeeding experiments.

(E, F) Correlation of total EE against locomotor activity in a representative mouse during fasting (E) and HD feeding (F).

(G, H) Schematic presentations of RMR, Ex and DIT in total EE.

# Figure 2

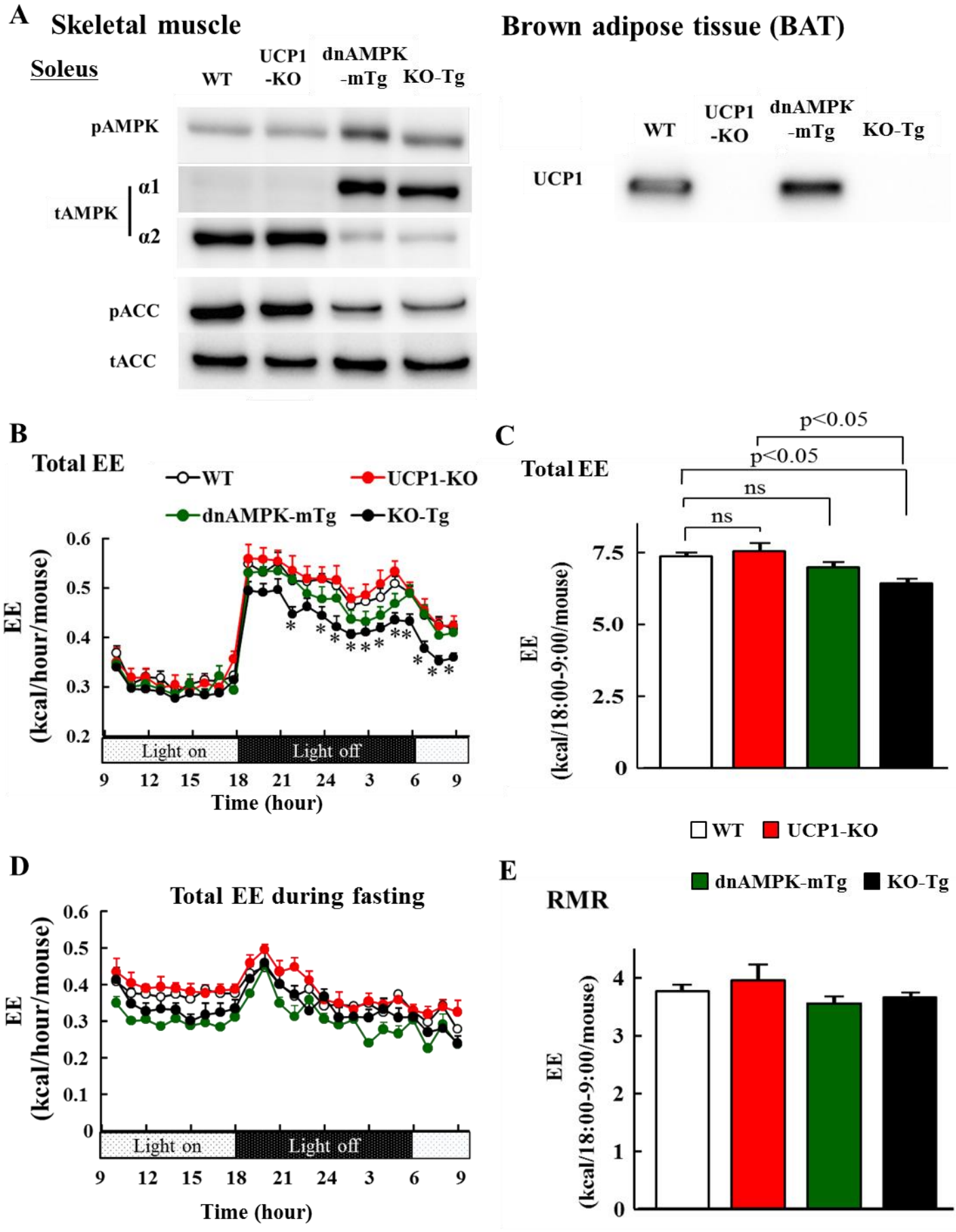
A
Skeletal muscle
Soleus
WT
UCP1 -KO
dnAMPK -mTg
KO-Tg
pAMPK
tAMPK
α1
α2
pACC
tACC
Brown adipose tissue (BAT)
UCP1
B
Total EE
WT
UCP1-KO
dnAMPK-mTg
KO-Tg
EE (kcal/hour/mouse)
Light on
Light off
Time (hour)
C
Total EE
p<0.05
p<0.05
ns
ns
EE (kcal/18:00-9:00/mouse)
D
Total EE during fasting
E
RMR

# Figure 2 (continued)

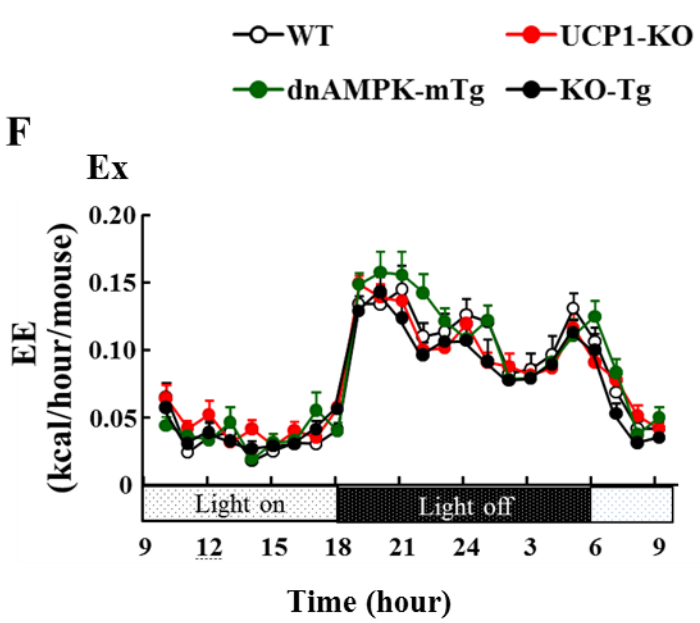


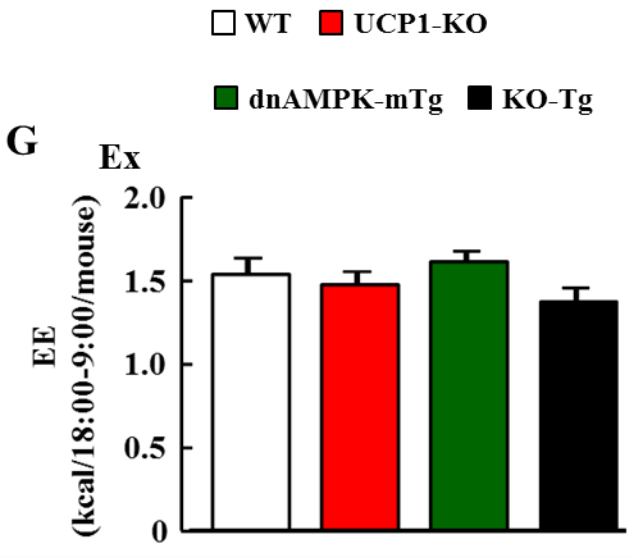


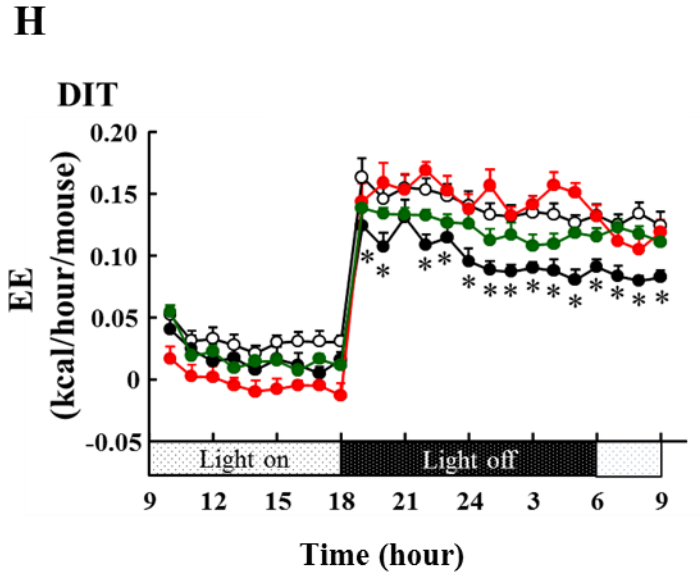


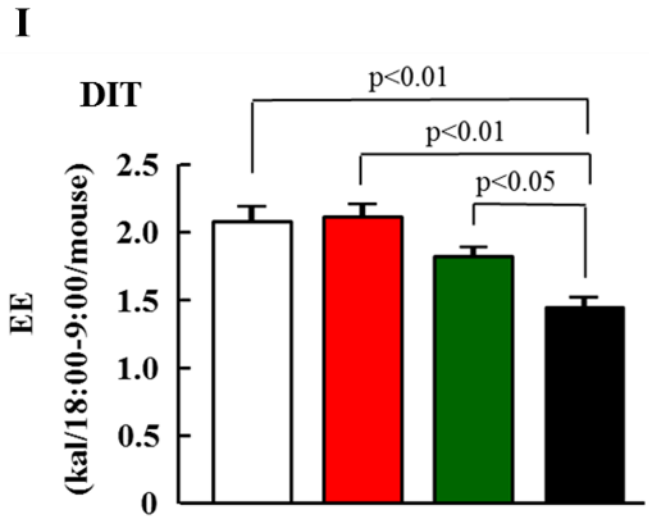

Figure 2. Decrease of total EE and DIT in KO-Tg mice but not in UCP1-KO or dnAMPK-mTg mice.

(A) Expression and phosphorylation of AMPK and ACC in soleus muscle, and expression of UCP1 protein in BAT.

(B) Total EE during HFD feeding at subthermoneutral room temperature (24ºC).

(C) Sum of total EE during HFD feeding from 18:00 to 9:00.

(D) Total EE during fasting.

(E) Sum to total EE during fasting from 18:00 to 9:00.

(F) Ex during HFD feeding.

(G) Sum of Ex during HFD feeding from 18:00 to 9:00.

(H) DIT during HFD feeding.

(I) Sum of DIT during HFD feeding from 18:00 to 9:00.

All quantitative data are mean ± SEM (n=9-10). Error bar represents the SEM.

*, $p<0.05$ vs WT mice.

# Figure 3

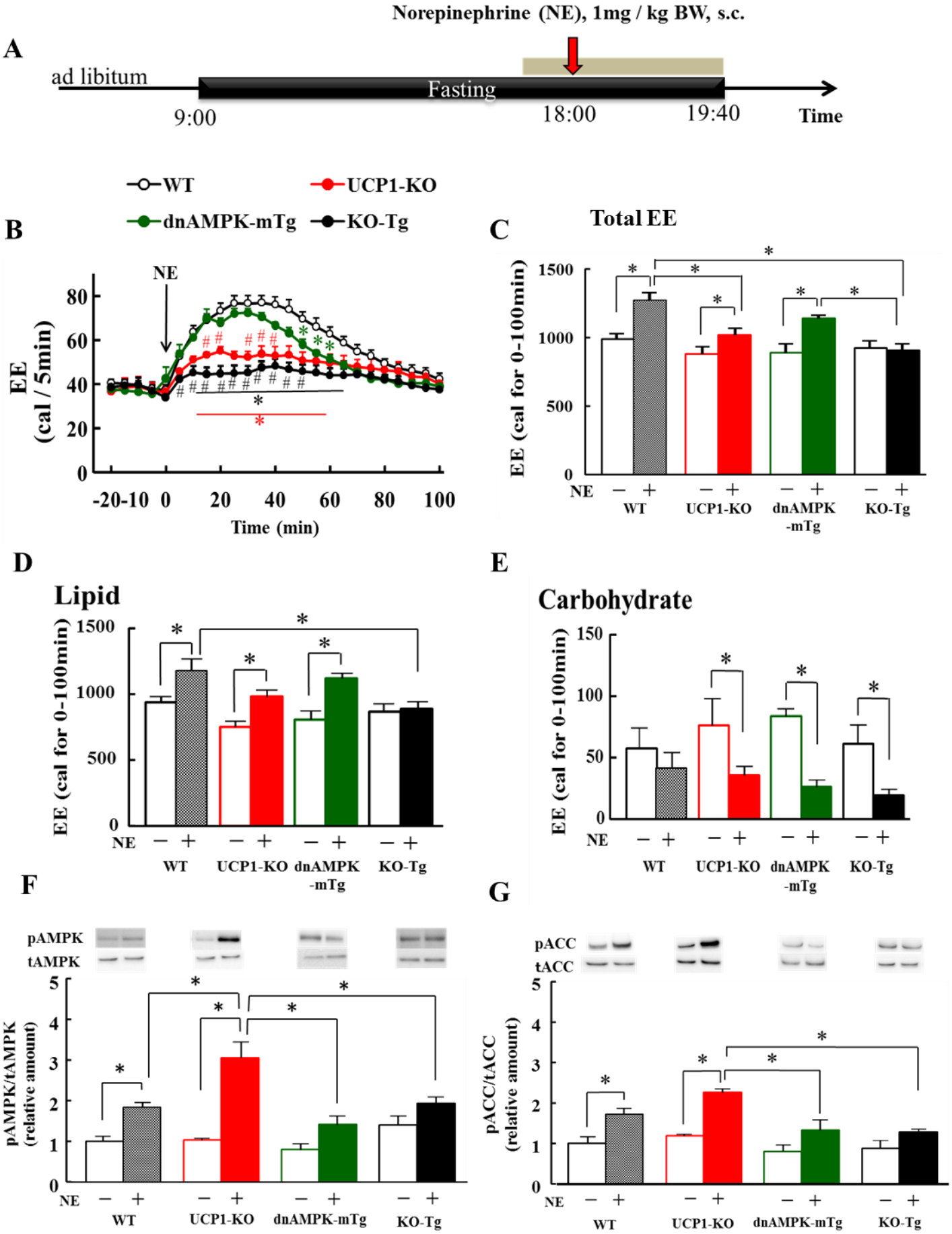
A
Norepinephrine (NE), 1mg / kg BW, s.c.
ad libitum
Fasting
9:00
18:00
19:40
Time
B
WT
UCP1-KO
dnAMPK-mTg
KO-Tg
NE
EE (cal / 5min)
Time (min)
C
Total EE
EE (cal for 0-100min)
NE
WT
UCP1-KO
dnAMPK -mTg
KO-Tg
D
Lipid
E
Carbohydrate
F
pAMPK
tAMPK
pAMPK/tAMPK (relative amount)
G
pACC
tACC
pACC/tACC (relative amount)

Figure 3. NE-induced change in total EE and phosphorylation of AMPK and ACC in soleus muscle.

(A) Experimental schedule for NE injection experiments.

(B) Change in total EE after NE injection.

*, $p<0.05$ vs WT mice. #, $p<0.05$ vs dnAMPK-mTg mice.

(C) Change in total EE after injection of NE (color bars) or saline (white bar).

(D, E) Lipid (D) and carbohydrate (E) oxidation after injection of NE (color bars) or saline (white bar).

(F, G) Phosphorylation of AMPK (F) and ACC (G) after injection of NE (color bars) or saline (white bar).

All quantitative data are mean ± SEM (n=5-8). Error bar represents the SEM. *, $p<0.05$ (C-G).

# Figure 4

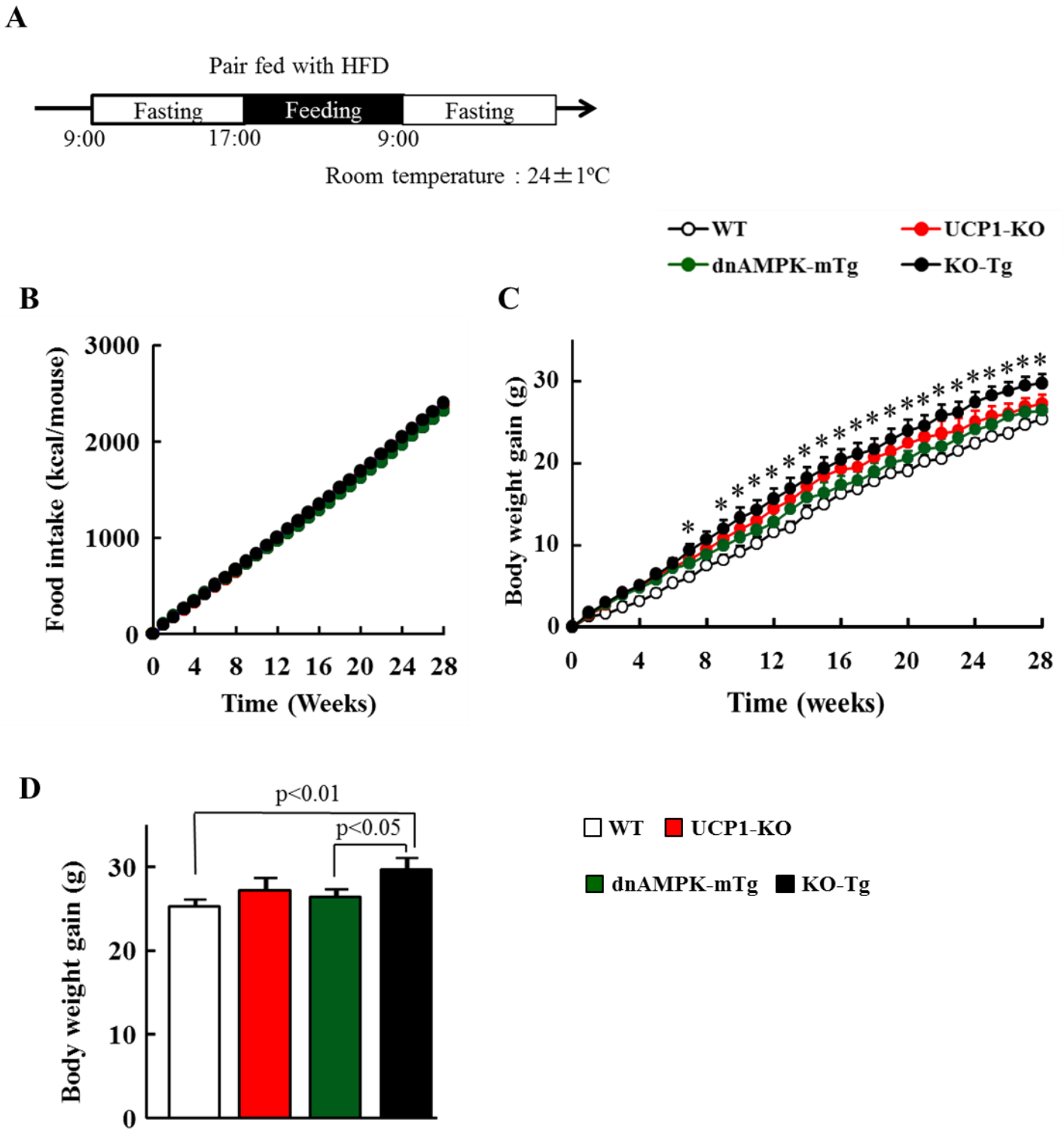
A
Pair fed with HFD
Fasting
Feeding
Fasting
9:00
17:00
9:00
Room temperature : 24±1ºC
WT
UCP1-KO
dnAMPK-mTg
KO-Tg
B
Food intake (kcal/mouse)
3000
2000
1000
0
0 4 8 12 16 20 24 28
Time (Weeks)
C
Body weight gain (g)
30
20
10
0
0 4 8 12 16 20 24 28
Time (weeks)
D
p<0.01
p<0.05
Body weight gain (g)
30
20
10
0
WT
UCP1-KO
dnAMPK-mTg
KO-Tg

Figure 4. Induction of obesity in KO-Tg mice at subthermonerutral room temperature.

(A) Pair-feeding of HFD with time-restricted schedule.

(B) Accumulated food intake.

(C) Body weight gain with HFD pair-feeding

(D) Body weight gain at 28 weeks.

All quantitative data are mean ± SEM (n=10-13). Error bar represents the SEM. *, $p<0.05$ vs WT mice.

# Figure 5

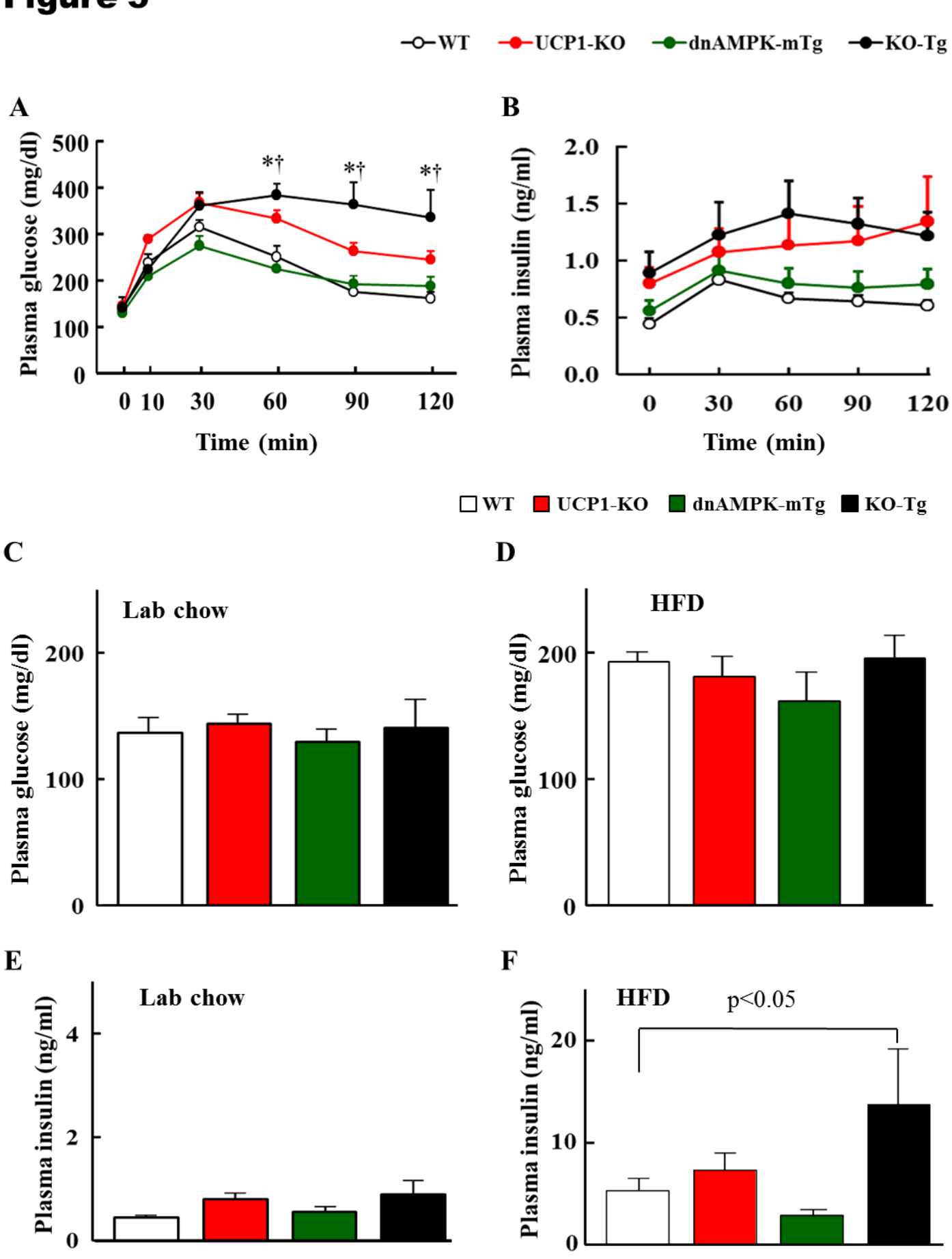
WT
UCP1-KO
dnAMPK-mTg
KO-Tg
A
Plasma glucose (mg/dl)
500
400
300
200
100
0
*†
*†
*†
0 10 30 60 90 120
Time (min)
B
Plasma insulin (ng/ml)
2.0
1.5
1.0
0.5
0.0
0 30 60 90 120
Time (min)
WT
UCP1-KO
dnAMPK-mTg
KO-Tg
C
Lab chow
Plasma glucose (mg/dl)
200
100
0
D
HFD
Plasma glucose (mg/dl)
200
100
0
E
Lab chow
Plasma insulin (ng/ml)
4
2
0
F
HFD
p<0.05
Plasma insulin (ng/ml)
20
10
0

# Figure 5 (continued)

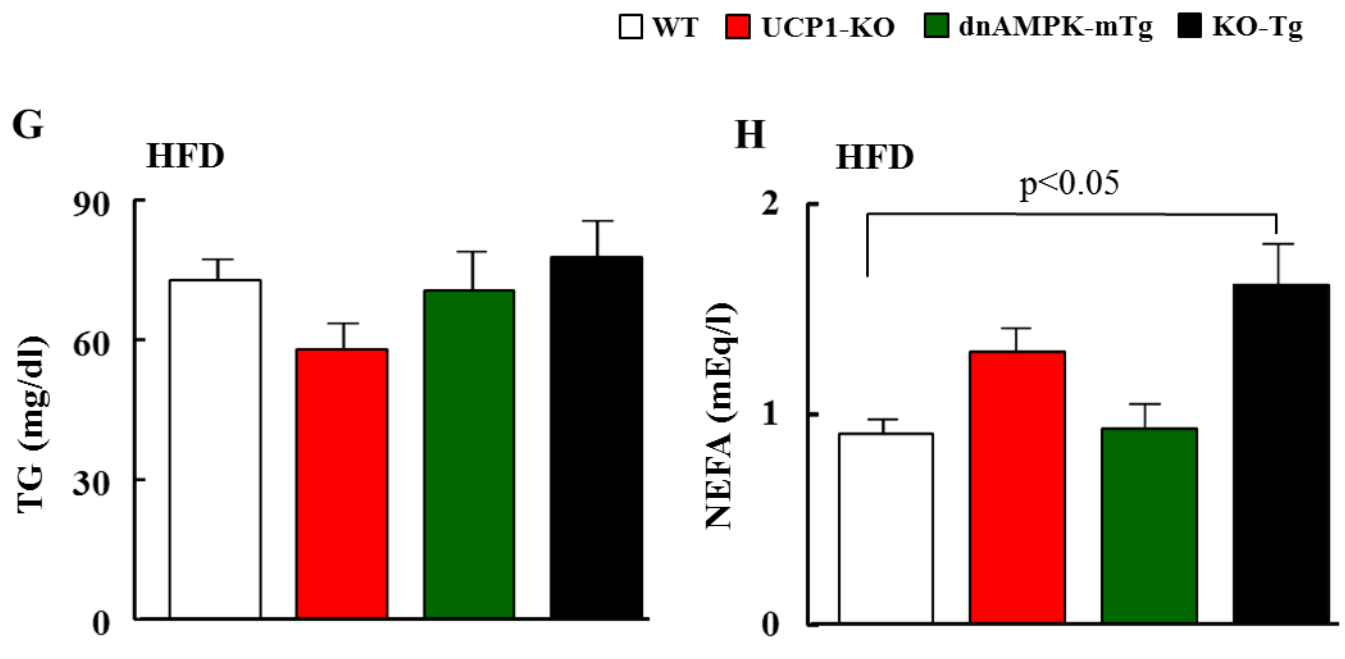

Figure 5. Impairment of glucose and lipid metabolism in KO-Tg mice.

(A, B) Plasma glucose and insulin concentrations during GTT in mice fed lab chow ad libitum.

(C, D) Plasma glucose concentrations in mice fed lab chow ad libitum (C) or pair-fed HFD with time-restricted schedule (D).

(E, F) Plasma insulin concentrations in mice fed lab chow ad libitum (C) or pair-fed HFD with time-restricted schedule (D).

(G, H) Plasma nonestrified fatty acid (NEFA) (G) and triglyceride (TG) (H) concentrations in mice pair-fed with time-restricted feeding schedule.

All quantitative data are mean ± SEM (n=5-10). Error bar represents the SEM. *, $p<0.05$ vs WT mice. †, $p<0.05$ vs dnAMPK-mTg mice.